Recent Research in Science and Technology 2012, 4(8): 114-116
ISSN: 2076-5061
Available Online: http://recent-science.com/

Sol gel synthesis and photoluminescence study of Eu^{3+} doped SnO_2

Namrata Bajpai[1], S.A. Khan[2], R.S. Kher[3], Namita Brahme[4], S.J. Dhoble[5]

[1]Lecturer, Department of Chemistry, NIT Raipur (C.G)
[2]Principal, Govt. Science Collage, NTPC Seepat, Bilaspur (C.G)
[3]Professor and HOD, Department of Physics, Govt. Science collage, Bilaspur (C.G).
[4]Reader, SOS in Physics and astrophysics, Pt. Ravishankar Shukla University Raipur, Chhattisgarh, India
[5]Associate Professor. Department of Physics. RTM, *Nagpur* University

Abstract
Tin oxide(IV) nanophosphor doped with europium had been prepared by sol-gel technique using $SnCl_4$ as precurser. XRD, IR, SEMand TEM analyses were used for characterization of SnO_2:Eu^{3+}. The XRD analysis shows that well crystallized tetragonal rutile SnO_2:Eu^{3+} can be obtained by this method and the crystal size was about 15-20nm as an average for the sample calcined at 400ºC for 2h. The evolution of the most important functional groups during the steps involved in this synthesis route is explained in view of the results obtained with FTIR and XRD. A spherical like morphology of the prepared SnO_2 nanoparticles was observed in the SEM and TEM studies. The SnO_2 nanoparticles show stable photoluminescence emission intensity at 612 nm ($^5D_0/^7F_2$) of the Eu^{3+} ions activated SnO_2 nanocrystals This paper discuss the mechanistic approach of origin of luminescence in SnO_2.

Keywords: Sol-gel polymerization, PL , Gelation time, SnO_2:Eu^{3+}.

INTRODUCTION

SnO_2 is a direct band gap n-type semiconductor (Eg=3.6 eV) and has been very extensively used for making sensors and optical devices [1–3]. Synthesis of SnO_2 nanoparticles has been reported by many authors and in most of the studies the synthesis temperature is above 350ºC [4–6]. It's optical (transparent for visible light and reflective for IR) and electrical properties, allied to good chemical and mechanical stability. It has been widely used for various catalytic applications, gas sensing, transparent conducting electrodes and liquid crystal displays, etc., [7-11]. Nanostructured SnO2 particles have been prepared by using different chemical methods such as precipitation, hydrothermal, sol-gel, gel-combustion and spray pyrolysis [12-20]. Among various methods, Sol-gel is well suited for production of nanostructured materials, because of its relatively low processing cost and the ability to control the grain size. The sol-gel process can roughly be defined as the conversion of a precursor solution into an inorganic solid by chemical means.

For example, Gu et al. [21] have reported the preparation of SnO_2 nanoparticles by sol–gel method using $SnCl_4.5H_2O$ and NH_4OH followed by heating over the temperature range of 400–600ºC. These particles showed luminescence around 400nm characteristic of oxygen vacancies present in the nanoparticles and its intensity was found to decrease with increase in heat treatment temperature. In general, during high temperature synthesis, the stabilizing ligands decompose leading to the aggregation of the particles, thereby resulting in poor dispersability in different solvents and decrease in luminescence. Generally, lanthanide ions like Eu^{3+}, Er^{3+}, etc., are incorporated in semiconductors to improve the luminescence efficiency by energy transfer process [22–27].

Since the shape, size, and dimensionality of semiconductors are vital parameters for their properties, developing a facile method to prepare important nanomaterials with well-defined structures is of great interest and importance. High-temperature treatment of lanthanide doped nanoparticles results in lanthanide ion clustering and subsequent phase separation. This leads to the decrease in the luminescence efficiency due to self-quenching. Luminescence studies on SnO_2: Eu nanopowders prepared by Sol-gel method at room temperature and calcined at 400ºC, have been reported by Fu et al. [28]. The average crystalline size of these particles varies from 15 to 20nm depending on heat treatment temperatures.

Excitation spectrum corresponding to 590nm emission from these nanoparticles, showed peaks characteristic of both Eu^{3+} and SnO_2 nanocrystal, and based on this result authors concluded that there is strong energy transfer from the SnO_2 nanocrystals to Eu^{3+} ions. The broad emission peaks observed around 400 and 460nm have been attributed to the emission from defects or traps present in the host SnO_2. Their properties depend on microstructure, impurities and size effects of particles.

A few papers [29–31] have been recently reported onrare-earth ions containing SnO_2 nanoparticles, which is the topic of the manuscript. They may find wide ranging applications such as micro-lasers, multicolor display and luminescent labels. Combining the promising optical properties of rare-earth ions and nanoparticles, in the form of coatings or thin films is important in fabrication of optical devices such as multicolor display and microlasers. In case of rare-earth ions, the electronic f–f transitions involve electrons which are localized in atomic orbital of the ions. Therefore, no size-dependent quantization effect from confinement of delocalized electrons is found of these transitions. However, confinement effects of semiconductor nanoparticles create photogenerated carriers may have an interaction with f-electrons which has important manifes-tations in influencing the optical properties.

EXPERIMENTAL PROCEDURE

Chemicals

The chemicals used in this study were tin(IV) chloride tetrahydrate ($SnCl_4.5H_2O$, Sciteg), ammonium hydroxide (NH_4OH

25%,Merck), sodium hydroxide (NaOH, R & M Chemicals) Europium oxide and ultra pure water obtained by SQ-Ultra Pure Water Purification System, Germany. All reagents were used as received without any further purification.

Synthesis of SnO_2 nanoparticles

Sol-gel route of synthesis is used for preparing tin oxide nanoparticles [32]. 2.94 g tin(IV) chloride was added to 50 mL ultra pure water in a round bottom flask and stirring was done for 20 min. A certain amount of ammonia solution (25%) was added into the mixture under a controlled feed rate of 0.01-0.1 mL min^{-1} and constant stirring. After 2 h of stirring, the sol was aged at room temperature for 24 h. The resulting gel was then washed with ethanol until the pH of the solution became 7. The gel was dried at 80ºC for 24 h in air, the obtained powder was ground using mortar and pestle and finally calcined at 400º C for 2 h.

For the Eu_2O_3 doped SnO_2 nanoparticles, the required amount (for 1.0 mol% Eu_2O_3) of $Eu(NO_3)_3.6H_2O$ was added to the aqueous solution of $SnCl_4.5H_2O$ and then followed the same procedure. The resulting product was then centrifuged and washed as above. Finally, the dried gel particles were annealed out at 400ºC for 2 h.

RESULT AND DISCUSSION

The formation of SnO_2 was confirmed with XRD results (Fig. 1). The molecular structure and composition of phosphors were characterized by Fourier Transform Infrared Spectroscopy FTIR (Fig. 2). IR spectra were recorded in the range of 400 to 4000 cm at room temperature using FTIR Spectrometer 1760X (Perkin Elmer) and compared with standard data. The sample was further characterized by SEM and TEM which shows its size as 15 nm (approx average).

The crystalline phases of annealed powders were identified by X-ray diffraction (XRD) using a Philips model PW-1730, powder X-ray diffractometer using a Cu Ka source (1.5418 A˚ radiation). Crystallite sizes (D,in A ˚) were estimated from the Scherrer equation. The excitation and emission spectra of SnO_2:Eu^{3+} ions were measured using a Perkin–Elmer LS55 Luminescence Spectrometer. All measurements were done at room temperature, using solid sample holder.

Fig. 1 2theta values are 26.8, 34.3 and 52.38, which are identified for SnO_2 phase (JCPDS card 41-1445). Similar results are obtained for 400 annealed pure SnO_2 samples. The crystallite sizes of these nanocrystals were calculated using the Scherrer's equation and our estimated average crystallite sizes of pure SnO_2:Eu^{3+} nanocrystals are 11nm (avg) at 400ºC, respectively. The major peaks at 29.1, 30.11 and 49.76 are due to Eu_2O_3 monoclinic phase (JCPDS Card 34–72).

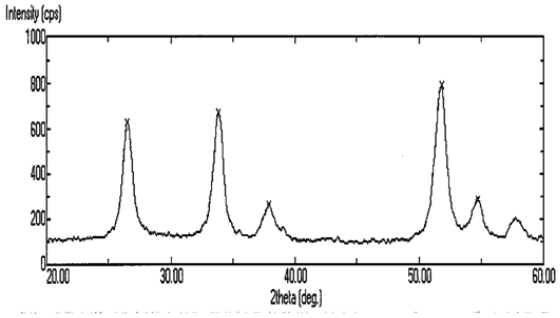

Fig 1. XRD of SnO_2

As-prepared SnO_2:Eu^{3+} powders exhibit an intense, very broad peak ranging from ca. 3600 to 2400 cm^{-1}, with two maximum at ca. 3380 and 3050 cm^{-1}, which may be due to the adsorbed water and NH3. After calcination, the peak at 3380cm^{-1} shift to higher wave numbers, while the peak at 3050cm-1 disappears. The band centered at ca. 1626cm^{-1} may also be related to water. Increasing the calcination temperature results in the decrease in the intensity of the water band, and after heating at 400ºC, the band attributed to NH_3 at around 3050cm^{-1} disappears. The low wave number region exhibits a strong vibration around 615 cm^{-1}, which can be assigned to ν(Sn–O–Sn) of the tin oxide framework [33].

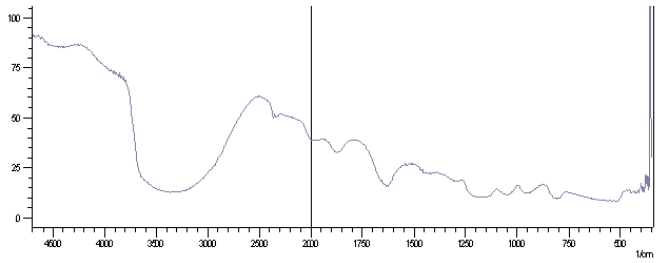

Fig 2. IR spectral analysis of SnO_2

The morphology and particle size of SnO2:Eu^{3+} was further investigated by SEM and TEM studies. From the SEM studies, Tin oxide nanoparticles are spherical and ellipsoidal morphology and the diameter of the nanoparticles was ca. 15 and 17nm (Shown in Fig.3). Moreover, some of the particles were aggregated. In this preparation method, the gel structure was maintained during the rutile SnO_2 nanoparticles formation process [34].

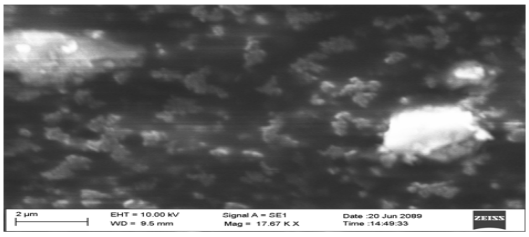

Fig 3. SEM analysis of SnO_2:Eu^{3+}

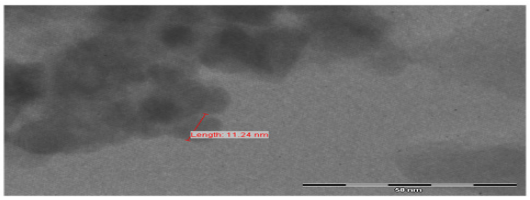

Fig 4. TEM analysis of SnO_2:Eu^{3+}

Figs. 4 (a, b, c, d) show the emission spectra for pure and Eu activated (2mole%,1.5mole%,1mole%,) SnO_2 nanoparticles. The strong emission bands at 390, 425, 484 and 540 nm are observed for SnO_2 nanoparticles (Figs. 4). The emission band at 390 nm can be attributed to electron transition mediated by defects levels in the band gap, such as oxygen vacancies ($^5D_0/^7F_1$) [36, 37]. The band at 425 nm is designated due to tin interstitials or dangling present in the SnO_2 nanocrystals [34, 35]. However, in case of Eu activated SnO_2 nanocrystals, the additional peaks at 612 nm ($^5D_0/^7F_2$) for doped sample (Figs 4. After 650 nm the emission is rare and it is supposed to be due to $^5D_0/^7F_2$ transition. It is believed that the energy transfer from SnO_2 nanocrystals to the Eu^{3+} ions is occurred in both the cases. The energy transfer from SnO_2 nanocrystals to Eu^{3+} ions is possible because the emission band at 390 nm for SnO_2 particles

are almost matching with the excitation band (392 nm) of Eu^{3+} ions.

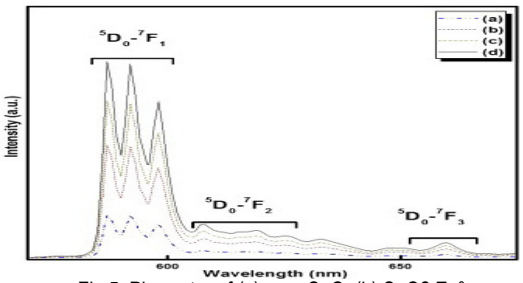

Fig 5. Pl spectra of (a) pure SnO_2 (b) SnO2:Eu^{3+}

Here, we can see the decrease in overall intensity of the SnO_2 emission drastically when the intensity of the 612 nm peak grows. This indicates that the emission energy of SnO_2 is consumed for the excitation of Eu^{3+} ions. It is known [36] that the enhanced luminescence occurs through the recombination of photo-generated carriers confined in nanoparticles and subsequent energy transfer to rare-earth ions. The energy transfer efficiency from nanocrystal to Eu^{3+} ions is estimated accordingly η_{et}=1- I/I_0, where I_0 is the total emission intensity of pure SnO_2 nanocrystals without europium and I corresponds to the emission intensity of SnO_2 nanocrsytals in presence of europium. The calculated energy transfer efficiencies for doped samples is 0.59. Comparison to commercially available highly efficient phosphors operating within this spectral range reveals a rough estimate of 5% for the overall quantum yield

CONCLUSION

Eu-doped SnO2 nanocrystalline powders were prepared by the sol–gel calcination method. The structure of the nanocrystalline powders is a rutile phase as seen by XRD analysis. The FTIR spectrum shows one absorption band containing two components at 613 $cm^{-1}$and 533 cm^{-1}, which arise from the stretching vibration of the O–Sn–O bond and the defect on the nanocrystalline surface, respectively. The emission spectra obtained by indirect excitation at 325 nm and direct excitations at 396 nm ($^5D_0$/$^7F_2$) and 466 nm ($^5D_0$/$^7F_1$) exhibit different emission line shapes. From the PL results, it can be concluded that the Eu^{3+} ions occupy different sites and Eu^{3+} ions located at different symmetry sites are selectively excited.

REFERENCES

[1] H. Ogawa, A. Abe, M. Nishikawa, S. Hayakawa, J. Electrochem. Soc. 128 (1981) 2020.

[2] Z.M. Jarzebski, J.P. Marton, J. Electrochem. Soc. 123 (1976) 299c.

[3] Z.M. Jarzebski, J.P. Marton, J. Electrochem. Soc. 123 (1976) 333c.

[4] F. Gu, S.F. Wang, M.K. Lu ¨, G.J. Zhou, D. Xu, D.R. Yuan, J. *Phys.Chem.* B 108 (2004) 8119.

[5] E.E. Nyein, U. Hommerich, J. Heikenfeld, D.S. Lee, A.J. Steckl, J.M.Zavada, *Appl. Phys. Lett.* 82 (2003) 1655.

[6] H. Zhang, X. Fu, S. Niu, G. Sun, Q. Xin, J. Lumin. 115 (2005) 7.

[7] K.L. Chopra, S. major, D.K. Pandya, *Thin Solid Films* 102,1 (1983) .

[8] C.Kilic, A. Zunger, Phys. Rev. Lett. 88, 095501 (2002).

[9] Z.W. Chen, J.K.L. Lai, C.H. Shek, *Phys. Rev.* B 70, 165314 (2004).

[10]A. Dieguez, A.R. Rodriguez, A. Vila, J.R. Morante, *J. Appl. Phys.* 90 (2001) 1550.

[11]T. Arai, *J. Phys. Soc. Jpn*. 15, 916 (1960).

[12]Gnanam S., Rajendran V., *Digest Journal of Nanomaterials and Biostructures,* 5, 3,699-704 2010.

[13]Sakka, S. and Kamiya, K*., J. Non-Cryst. Solids*, 1982, 48, 31.

[14]Sakka, S. and Kozuka, H*., J. Non-Cryst. Solids* , 1988, 100, 142.

[15]Kamiya, K., Yoko, T. and Suzuki, H., *J. Non-Cryst. Solids* 1987, 93, 407.

[16]Kamiya, K., Iwamoto, Y., Yoko, T. and Sakka, S., *J. Non-Cryst.* Solids, 1988, 100, 195.

[17]Pouxviel, J.C., Boilot, J.P., Beloeil, J.C. and Lallemand, J.Y. "NMR Study of the sol/gel polymerization", *J. Non-Cryst. Solids* 1987, 89, 345.

[18]Pouxviel, J.C. and Boilot, J.P., *J. Non-Cryst. Solids* 1987, 94, 374.

[19]Rakov N, Maciel G S, Lozano W B and Ara´ ujo C B 2006 Appl. *Phys. Lett.*88081908

[20]Bai X, Song H, Pan G, Liu Z, Lu S, Di W, Ren X, Lei Y, Dai Q and Fan L 2006Appl. Phys. Lett.8814310

[21]F. Gu, S.F. Wang, M.K. Lu ¨, Y.X. Qi, G.J. Zhou, D. Xu, D.R. Yuan, *Opt. Mater*. 25 (2004) 59.

[22]N. Hamelin, P.G. Kik, J.F. Suyver, K. Kikoin, A. Polman, A. Scho¨necker, F.W. Saris*, J. Appl. Phys.* 88 (2000) 5381.

[23]S. Okamoto, M. Kobayashi, Y. Kanemitsu, T. Kushida, *Phys. Status Solidi* B 229 (2002) 481.

[24]W. Chen, J.-O. Malm, V. Zwiller, Y. Huang, S. Liu, R. Wallenberg, J.-O. Bovin, L. Samuelson, *Phys. Rev.* B 61 (2000) 11021.

[25]X. Fu, H. Zhang, S. Niu, Q. Xin, *J. Solid State Chem*. 178 (2005) 603.

[26]J.D. CaStillo, V.D. Rodriguez, A.C. Yanes, J. Mendez-Ramos, M.E. Torres, *Nanotechnology* 16 (2005) S300.

[27]P. G. Harrison and A. Guest, *J. Chem. Soc., Faraday Trans*. 83, 3383 (1987).

[28]Colby, M.W., Osaka, A. and Mackenize, J.D., *J. Non-Cryst. Solids* 1986, 82, 37.

[29]F. Gu, S.F. Wang, C.F. Song, M.K. Lu, Y.X. Qi, G.*J. Zhou*, D. Xu, D.R. Yuan, Chem. *Phys. Lett.* 372 (2003) 451.

[30]F. Gu, S.F. Wang, M.K. Lu, Y.X. Qi, G.J. Zhou, D. Xu,

[31]D.R. Yuan, *Opt. Mater.* 25 (2004) 59.

[32]M. Nogami, T. Enomoto, T. Hayakawa*, J. Lumin.* 97 (2002) 147.

[33]You H and Nogami M 2004*J. Appl. Phys.*952781

[34]Maneva N, Kynev K, Grigorov L and Lijutov L *1997J. Mater. Sci. Lett.*161037

[35]Li J, Wang X, Watanabe K and Ishigaki T 2006 *J. Phys. Chem.* B1101121